

# Loss-enabled sub-Poissonian light generation in a bimodal nanocavity

Arka Majumdar,<sup>\*</sup> Michal Bajcsy, Armand Rundquist, and Jelena Vučković

*E.L.Ginzton Laboratory, Stanford University,  
Stanford, CA, 94305*

## Abstract

We propose an implementation of a source of strongly sub-Poissonian light in a system consisting of a quantum dot coupled to both modes of a lossy bimodal optical cavity. When one mode of the cavity is resonantly driven with coherent light, the system will act as an efficient photon number filter, and the transmitted light will have a strongly sub-Poissonian character. In addition to numerical simulations demonstrating this effect, we present a physical explanation of the underlying mechanism. In particular, we show that the effect results from an interference between the coherent light transmitted through the resonant cavity and the super-Poissonian light generated by photon-induced tunneling. Peculiarly, this effect vanishes in the absence of the cavity loss.

An optical cavity containing a strongly coupled quantum emitter, such as an atom or a quantum dot (QD), constitutes a system in which an optical nonlinearity is present even at a single photon level [1–3]. The eigen-energies of this coupled system form an anharmonic ladder, which gives rise to phenomena like photon blockade and photon-induced tunneling [4–7]. In photon blockade, coupling of a single photon to the system hinders the coupling of the subsequent photons, whereas in photon-induced tunneling, coupling of initial photons favors the coupling of the subsequent photons. In an experiment, the signature of blockade or tunneling is observed by measuring the second order autocorrelation function  $g^{(2)}(0)$ ;  $g^{(2)}(0) < 1$  ( $> 1$ ) demonstrate the sub-Poissonian (super-Poissonian) photon statistics of the transmitted light and indicate that the system is in a photon blockade (tunneling) regime.

Photon blockade can be used to route photons in a quantum photonic circuit [8], or to mimic interacting bosons for efficient simulation of complex quantum phase transitions [9–11]. While most of the recent experiments focus on photon blockade with a single two level system and a single cavity [4–7], there have been several theoretical proposals predicting photon blockade in systems based on multi-level atoms in a cavity [12] and on a quantum dot interacting with a pair of proximity-coupled nanocavities [13, 14] or wave-guides [15].

The cavity quantum electrodynamic (cQED) systems where photon blockade could be studied depend on three important rate quantities: the coherent coupling strength between the atomic system and the cavity  $g$ , cavity field decay rate  $\kappa$  and the dipole decay rate  $\gamma$ . In all aforementioned proposals, the photon blockade occurs when the coherent interaction strength is larger than the loss rates in the system. In fact, the limit of  $g/\kappa, g/\gamma \rightarrow \infty$  results in vanishing overlap between the energy eigen-states of the anharmonic ladder, which in turn leads to a perfect photon blockade ( $g^{(2)}(0) = 0$ ). In a solid state optical system based on a photonic-crystal cavity with an embedded single QD as the two-level system, the condition  $g \gg \gamma$  is generally easy to satisfy. However, achieving the condition of  $g \gg \kappa$ , which requires a high quality (Q) factor of the cavity, is generally difficult due to fabrication challenges. As a result, even the best photon blockade with a QD embedded in a solid-state nanocavity reported so far in the literature gives a second order correlation  $g^{(2)}(0) \sim 0.75$  [7]. Though a proposal based on a QD interacting with a photonic molecule (a pair of coupled cavities) predicts efficient blockade even for cavities with easily achievable Q factors [13, 14], the suggested scheme requires both individual addressability of each cavity and a

large coupling strength between the two cavities. Since nanophotonic cavities are generally coupled via spatial proximity, large coupling poses a major challenge for achieving individual addressability (see Appendix).

In this paper, we propose a different approach for generation of strongly anti-bunched light which employs a bimodal cavity with both of its modes coupled to a QD. We will show that in this approach the cavity loss is actually crucial for achieving the effect, as opposed to photon blockade systems introduced so far in which the cavity loss plays a negative role. Specifically, the effect does not occur in our system in the limit of  $g/\kappa \rightarrow 0$ , which is intuitively expected, as this is what also happens for the cases of blockade in a single cavity with strongly coupled QD and in a photonic molecule. However, for  $g/\kappa \rightarrow \infty$ , the proposed system fails to generate sub-Poissonian light, in contrast with the single cavity with a strongly coupled QD, where a perfect photon blockade occurs in such limit. Here, we provide an intuitive explanation of how a balance between the coherent QD-cavity interaction and the decay of the cavity field is required to achieve strong sub-Poissonian output photon stream. Additionally, we analyze the nanophotonic platform for possible experimental realization of this effect.

In a conventional strongly coupled QD-cavity system, a QD interacts with a single cavity mode (Fig. 1a). In a bimodal cavity, the QD is coupled to both cavity modes (with photon annihilation operators  $a$  and  $b$ ) although there is no direct coupling between the two modes (Fig. 1b). Assuming the cavity modes are degenerate and the QD is resonant with both of them, the Hamiltonian  $\mathcal{H}$  describing such a system (in a frame rotating at the frequency of the laser driving the cavity mode  $a$ ) is:

$$\begin{aligned} \mathcal{H} = & \Delta(a^\dagger a + \sigma^\dagger \sigma + b^\dagger b) + g_a(a^\dagger \sigma + a \sigma^\dagger) \\ & + g_b(b^\dagger \sigma + b \sigma^\dagger) + \mathcal{E}(a + a^\dagger) \end{aligned} \quad (1)$$

Here,  $\sigma$  is the QD lowering operator,  $g_a$  and  $g_b$  are the coupling strengths between the QD and the two cavity modes,  $\mathcal{E}$  denotes strength of the driving laser and  $\Delta$  is the detuning between the driving laser and the cavity modes. The loss in the system is incorporated in the usual way by using the Master equation (see Appendix). The numerical calculations are performed using the integration routines provided in the quantum optics toolbox [16]. Fig. 1c shows the transmitted light collected from the driven cavity ( $\kappa \langle a^\dagger a \rangle$ ) for both single (dashed line) and double mode cavities (solid line). The cavity output is qualitatively similar

for both cases, and the split resonance is caused by coupling of the QD to the cavity and creation of polaritons. For the single mode cavity, the two polaritons are separated by  $2g$ , while for the bimodal cavity, the separation is  $2\sqrt{2}g$  due to the presence of two modes, as will be explained later. Increased cavity transmission at  $\Delta = 0$  for the bimodal case is also due to the presence of two modes. However, the second-order autocorrelation function of the cavity transmission  $g^{(2)}(0) = \frac{\langle a^\dagger a^\dagger a a \rangle}{\langle a^\dagger a \rangle^2}$  are strikingly different for two cases (Fig. 1d). For the single mode cavity, one observes photon blockade ( $g^{(2)}(0) < 1$ ), when the driving laser is tuned to the frequency of the polariton,  $\Delta \approx \pm g$ . For the bimodal cavity, sub-Poissonian statistics is observed at three different detunings:  $\Delta \approx \pm\sqrt{2}g$  and  $\Delta = 0$ . The weak sub-Poissonian light ( $g^2(0) \sim 0.95$ ) at  $\Delta \approx \pm\sqrt{2}g$  is comparable to that observed in the single mode cavity, and it arises from the same mechanism. At  $\Delta = 0$ , the sub-Poissonian character is much stronger ( $g^2(0) \sim 0.4$ ), and it is this regime in the bimodal cavity that we will focus on. Note that the sub-Poissonian character observed at this frequency of the driving laser cannot be explained by the anharmonic nature of the ladder alone. In fact, in the energy structure of the coupled QD and the bimodal cavity, we find an available state always at this empty cavity frequency (see Appendix).

To further illustrate the difference between the photon blockade in a single mode cavity and the effect we observe in a bimodal cavity, we perform numerical simulations for a range of coupling strengths  $g$  and the cavity field decay rates  $\kappa$  in both systems. Using these simulations, we obtained the values of  $g^{(2)}(0)$  for the transmitted light for a single mode cavity (laser tuned to one of the polaritons, i.e.,  $\Delta = g$ ) and for a double mode cavity (the laser tuned to the bare cavity frequency, i.e.,  $\Delta = 0$ ). Fig. 2a,b shows  $g^{(2)}(0)$  as a function of  $g$  and  $\kappa$ . For a single mode cavity, blockade appears at high  $g$  and low  $\kappa$ , as generally expected for any photon blockade systems (Fig. 2a). However, for a bimodal cavity, the effect disappears and the transmitted photon output returns to Poissonian whenever  $g$  and  $\kappa$  are disproportionate (i.e.,  $g/\kappa \rightarrow 0$  or  $g/\kappa \rightarrow \infty$ ). A strongly sub-Poissonian output can be observed when  $g$  and  $\kappa$  are comparable. Again, this result cannot be explained just by the anharmonicity of the ladder of energy eigenstates.

To understand the origin of the strongly sub-Poissonian light transmitted through a bimodal cavity, we transform the system's Hamiltonian to a different cavity mode basis:  $\alpha = (a + b)/\sqrt{2}$  and  $\beta = (a - b)/\sqrt{2}$ . The Hamiltonian  $\mathcal{H}$  can be written (assuming

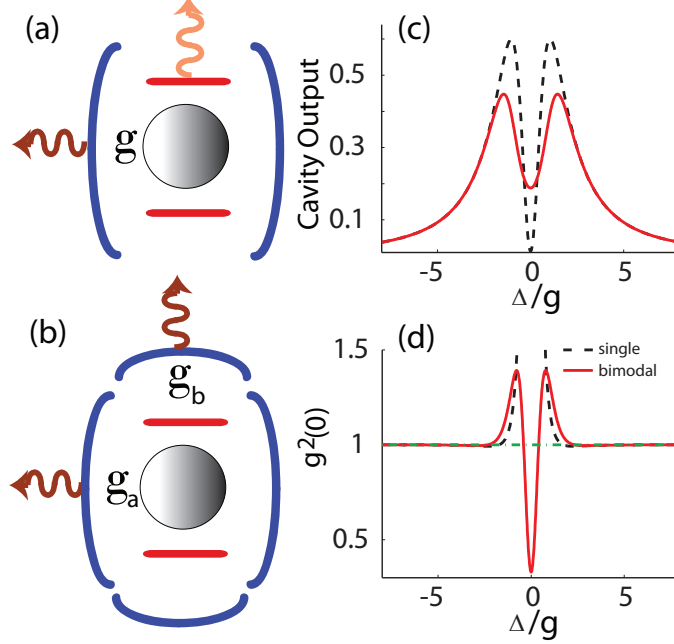


FIG. 1: (color online) (a) Schematic of a QD coupled to a single mode cavity, with a coupling strength of  $g$ . (b) Schematic of a bimodal cavity with a coupled QD. The two cavity modes are not directly coupled to each other. However, both of them are coupled to the QD with interaction strength  $g_a$  and  $g_b$ . (c) The cavity output  $\kappa\langle a^\dagger a \rangle$  as a function of the driving laser detuning  $\Delta$  from the empty cavity resonance both for a single mode cavity (dashed line) and the bimodal cavity (solid line). The split resonance observed is due to the coupled QD. (d) Second order autocorrelation  $g^{(2)}(0)$  function calculated for the collected output of the driven mode for a single mode (dashed line) and bimodal cavity (solid line). The green dashed line marks the Poissonian statistics of a coherent state. For bimodal cavities we assumed identical interaction strength and cavity decay rates for two modes. Parameters used for the simulations: QD-cavity interaction strength  $g/2\pi = g_a/2\pi = g_b/2\pi = 10$  GHz, cavity field decay rate  $\kappa/2\pi = 20$  GHz, dipole decay rate  $\gamma/2\pi = 1$  GHz, and driving laser strength  $\mathcal{E}/2\pi = 1$  GHz.

$g_a = g_b = g$ ) as  $\mathcal{H} = \mathcal{H}_1 + \mathcal{H}_2$  with

$$\mathcal{H}_1 = \Delta(\alpha^\dagger \alpha + \sigma^\dagger \sigma) + \sqrt{2}g(\alpha^\dagger \sigma + \alpha \sigma^\dagger) + \frac{\mathcal{E}}{\sqrt{2}}(\alpha + \alpha^\dagger) \quad (2)$$

describing a driven single mode cavity coupled to a QD with a strength of  $\sqrt{2}g$  and

$$\mathcal{H}_2 = \Delta\beta^\dagger \beta + \frac{\mathcal{E}}{\sqrt{2}}(\beta + \beta^\dagger) \quad (3)$$

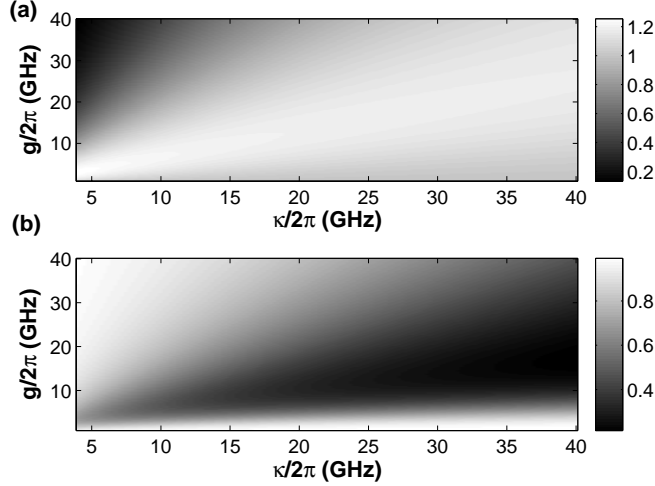


FIG. 2: (a) Second order autocorrelation  $g^{(2)}(0)$  for the conventional photon blockade in a single mode cavity as a function of the QD-cavity coupling strength  $g$  and cavity field decay rate  $\kappa$ .  $g^{(2)}(0)$  decreases with increasing value of  $g/\kappa$ , as expected, as a result of reduced overlap of energy eigenstates in the anharmonic ladder. (b)  $g^{(2)}(0)$  for the bimodal cavity as a function of  $g$  and  $\kappa$ .  $g^{(2)}(0)$  is calculated for the output of the mode  $a$ , i.e., photons leaking from the mode  $a$ . We observe that  $g^{(2)}(0)$  tends to go to 1 (Poissonian output) when  $g/\kappa \rightarrow 0$  or  $\infty$ . However, we can observe very low  $g^{(2)}(0)$  even when the QD is not strongly coupled to the two cavity modes ( $g < \kappa/2$ ).

describing a driven empty cavity mode. Both cavities are driven at the bare cavity resonances. We monitor  $a = (\alpha + \beta)/\sqrt{2}$  which, in the transformed basis, is equivalent to the output from two cavities: one with a coupled QD ( $\alpha$ ) and the other empty ( $\beta$ ), combined in a beam-splitter. Fig. 3a shows the transmitted cavity output for three different cases: cavity  $\alpha$  alone, cavity  $\beta$  alone and the combined output. Note the polariton peaks in the combined output at  $\pm\sqrt{2}g$  and increased transmission of light at zero detuning due to the empty cavity.

The cavity transmission with a strongly coupled QD driven at the cavity resonance is super-Poissonian due to photon-induced tunneling [6] ( $\alpha$  in Fig. 3b). In this regime, the coupling of initial photons into the system is inhibited by the absence of the dressed states at this frequency. However, once the initial photon is coupled, the probability of coupling subsequent photons is increased as higher order manifolds in the ladder of dressed states are reached via multiphoton processes. In our system, as a result of broadening of the dressed states, at empty cavity resonance one can excite multiple higher order manifolds.

Hence, the light transmitted through a cavity in the photon-induced tunneling regime is a superposition of Fock states with small photon numbers and a strong presence of the vacuum state. As a result, the photon statistics of this light is super-Poissonian [6]. On the other hand, the empty cavity transmission ( $\beta$  in Fig. 3 b) is a purely Poissonian coherent state. When the outputs of these two cavities are combined on a beam-splitter ( $a = (\alpha + \beta)/\sqrt{2}$  in Fig. 3 b), the output shows sub-Poissonian character somewhat similar to the photon-added coherent states [17, 18]. However, for efficient generation of sub-Poissonian light, one needs comparable transmitted light intensity from both cavities, which calls for a balance between the cavity loss  $\kappa$  and QD-cavity nonlinear interaction strength  $g$ . Using this effective model, the somewhat unusual dependence of  $g^{(2)}(0)$  on  $g$  and  $\kappa$  can now be explained. When  $g/\kappa \rightarrow 0$ , the coupled system is linear and both of the equivalent cavities transmit just coherent light. On the other hand, although photon-induced tunneling does happen in the limit  $g/\kappa \rightarrow \infty$ , the amount of super-Poissonian light transmitted through the cavity  $\alpha$  is so small (as the dressed states separation in the ladder is so large that it is impossible to couple photons at energies between them) that its interference with the coherent light from the empty cavity  $\beta$  will still result in light with Poissonian statistics. To generate enough super-Poissonian light via photon-induced tunneling in cavity  $\alpha$  to affect the coherent light from the empty cavity  $\beta$ , a moderate dot-cavity interaction strength  $g$  is required.

Finally, we discuss the nanophotonic platform that can be used to implement our proposal. A photonic-crystal cavity with  $C_6$  symmetry can support two degenerate cavity modes with orthogonal polarizations [19]. The two cavity modes are thus not coupled to each other (since their polarizations are orthogonal), and can be easily addressed independently by a laser. At the same time, a QD can be coupled to both cavity modes, if it is placed spatially at the center of the cavity with its dipole moment aligned at  $45^\circ$ -angle to the polarizations of both modes.

Two potential issues can arise from fabrication imperfections in a realistic system: a frequency difference  $\Delta_{ab}$  between the two cavity modes and a mismatch between the QD coupling strengths  $g_a$  and  $g_b$  to each mode. These issues can be seen in the preliminary experimental results shown in the Appendix. To examine the robustness of the proposed scheme against these imperfections, we plot their effects on  $g^{(2)}(0)$  in Fig. 4. Fig. 4a shows the numerically calculated  $g^{(2)}(0)$  as a function of the detuning  $\Delta_{ab}$ . We observe that the sub-Poissonian character of the transmitted light vanishes when  $\Delta_{ab} \geq \kappa$ . This negative

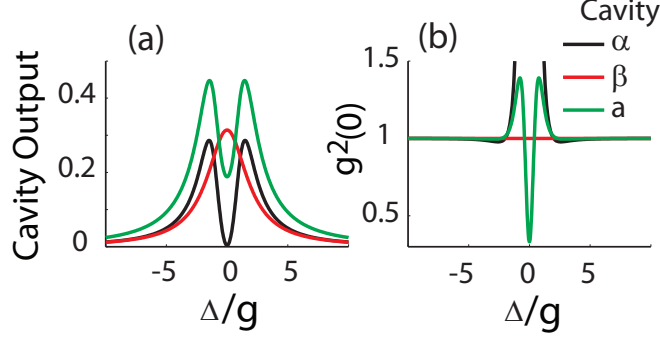


FIG. 3: (color online) (a) Cavity output for an empty cavity  $\beta$  and another cavity  $\alpha$  coupled to a QD with a coupling strength of  $\sqrt{2}g$ . The combined output of these two produces the output from the bimodal cavity  $a$ . (b)  $g^{(2)}(0)$  for these three cases: the empty cavity  $\beta$  gives Poissonian light; the cavity  $\alpha$  with coupled QD gives super-Poissonian light due to photo-induced tunneling [6] (the black curve goes to infinity at  $\Delta = 0$ ); the combined output  $a$  provides sub-Poissonian light. Parameters for the simulation:  $g/2\pi = 10$  GHz,  $\kappa/2\pi = 20$  GHz,  $\gamma/2\pi = 1$  GHz and  $\mathcal{E}/2\pi = 1$  GHz.

effect of frequency difference of the two modes can be balanced simply by increasing the cavity decay rate  $\kappa$ , i.e., by lowering the cavity quality factor. This results in an increase of the frequency overlap between the two modes and makes the degeneracy of the two modes more robust. The effects of this improvement outweigh the penalty incurred on the system's performance by reducing the  $\frac{g}{\kappa}$  ratio, and we can see in Fig. 4a that a strongly anti-bunched output can still be produced. Additionally, we analyze the performance of the system as a function of the ratio  $g_b/g_a$ , where  $g_b$  and  $g_a$  are the QD coupling strengths with the cavity modes  $a$  and  $b$  assuming mode  $a$  is coherently driven. It can be shown from the effective model that at a large  $g_b/g_a$  ratio, we essentially drive only the empty cavity  $\beta$  and the photon statistics are Poissonian. Similarly, at a small  $g_b/g_a$  ratio, we drive only the cavity  $\alpha$  with coupled QD and the photon statistics are super-Poissonian due to photo-induced tunneling (see Appendix). When  $g_b/g_a \sim 1$ , we meet the optimal condition of interference between the coherent state and super-Poissonian state to generate light with sub-Poissonian photon statistics. This can be seen in the numerical simulations of  $g^{(2)}(0)$  as a function of  $g_b/g_a$  in Fig. 4b. The system performance is insensitive to the actual value of  $g_a$  for a relatively large range, as long as the ratio  $g_b/g_a$  is maintained. At the same time, we can see that the lowest value of  $g^{(2)}(0)$  is achieved for the ratio of coupling strengths of



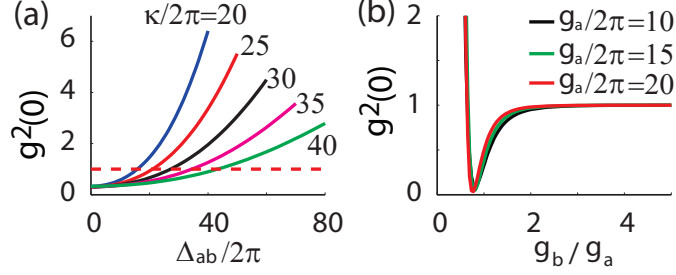


FIG. 4: (color online)(a) Second order autocorrelation  $g^{(2)}(0)$  of the cavity transmission, as a function of the relative detuning  $\Delta_{ab}$  between two cavity modes for different cavity field decay rate  $\kappa = \kappa_a = \kappa_b$ . The quality of the sub-Poissonian photon stream in the transmitted output degrades with increasing detuning, which can be compensated by increasing  $\kappa$ , while maintaining low  $g^{(2)}(0)$ . For these simulations we assume  $g_a/2\pi = g_b/2\pi = 10$  GHz. (b) Second order autocorrelation  $g^{(2)}(0)$  of the cavity transmission as a function of the ratio  $g_b/g_a$  for different  $g_a$ . The transmitted light behaves like a coherent state at high  $g_b/g_a$  ratio and like a super-Poissonian state generated via photo-induced tunneling at low  $g_b/g_a$  ratio. In between, when  $g_b/g_a \sim 1$ , we observe strong sub-Poissonian output. Here,  $\kappa/2\pi = 20$  GHz for both cavity modes.

$g_b/g_a \sim 0.8$ . We note that, this ratio depends on the driving strength of the laser, and can be related to the requirement of the similar cavity transmission from the cavities  $\alpha$  and  $\beta$ .

In summary, we introduced a scheme for generation of sub-Poissonian light in a cQED system with a bimodal cavity and provided a theoretical and numerical analysis of its performance. For similar system parameters, the bimodal cavity can provide much better sub-Poissonian character of the transmitted photon stream ( $g^{(2)}(0) \rightarrow 0$ ) compared to a single mode cavity ( $g^{(2)}(0) \sim 0.9$ ). The proposed effect happens due to interference between a coherent state and a super-Poissonian state generated by photon-induced tunneling, and a balance between the nonlinearity and the loss of the system is required to observe it. Moreover, the effect disappears in the absence of the cavity loss ( $g/\kappa \rightarrow \infty$ ). This interplay between loss and nonlinearity has a great potential to be exploited for design of realistic coupled cavity arrays for efficient quantum simulation.

The authors acknowledge financial support provided by DARPA, ONR, NSF and the ARO. A.R. is also supported by a Stanford Graduate Fellowship.

### **Eigen-structure of the quantum dot coupled to a bimodal cavity with loss:**

The Hamiltonian  $\mathcal{H}$  describing the coupled system is given by

$$\mathcal{H} = \Delta(a^\dagger a + \sigma^\dagger \sigma + b^\dagger b) + g_a(a^\dagger \sigma + a \sigma^\dagger) + g_b(b^\dagger \sigma + b \sigma^\dagger) + \mathcal{E}(a + a^\dagger) \quad (4)$$

To incorporate the loss in the system, we use a Master equation approach. The lossy dynamics of the quantum system are governed by

$$\frac{d\rho}{dt} = -i[H, \rho] + 2\kappa_a \mathcal{L}[a] + 2\kappa_b \mathcal{L}[b] + 2\gamma \mathcal{L}[\sigma]. \quad (5)$$

Here,  $\rho$  is the density matrix of the coupled QD-cavity system,  $2\gamma$ ,  $2\kappa_a$  and  $2\kappa_b$  are the QD spontaneous emission rate and the cavity population decay rates, and we neglect any non-radiative decay of the QD exciton. Finally,  $\mathcal{L}[D] = D\rho D^\dagger - \frac{1}{2}D^\dagger D\rho - \frac{1}{2}\rho D^\dagger D$  is the Lindblad operator corresponding to a collapse operator  $D$ .

Although the lossy dynamics describes the system in a more realistic way, a great deal of information can be obtained just from the coherent dynamics of the system, especially from the eigen-structure of the combined system. In fact, the explanation of photon blockade in the usual case of a two level system coupled to a single mode cavity relies mostly on the anharmonic ladder structure. This system is well-described by the Jaynes Cummings Hamiltonian, and the energy eigenstates are grouped in two-level manifolds with eigen-energies given by  $\pm g\sqrt{n}$  (for a resonant dot-cavity system), where  $n$  is the number of energy quanta in the coupled QD-cavity system. The eigenstates can be written as:

$$|n, \pm\rangle = \frac{|g, n\rangle \pm |e, n-1\rangle}{\sqrt{2}} \quad (6)$$

This anharmonicity gives rise to photon blockade when the driving laser is tuned to the polariton frequencies. In a similar manner, one can diagonalize the Hamiltonian for the bimodal cavity QED system. However, in contrast to the Jaynes-Cummings Hamiltonian, the matrix size for a specific number of quanta present in the bimodal cavity system is not fixed. In fact, for  $n$  quanta, the total number of bare basis states is  $2n + 1$ . In the Jaynes-Cummings Hamiltonian, the number of basis states is always 2, namely  $|e, n-1\rangle$  and  $|g, n\rangle$  for  $n$  quanta present in the system. From the symmetry of the coupled system, we find that the summation of the eigen-energies of the matrix (trace of the matrix) with  $n$  quanta is zero. As there is an odd number of eigen-values, by symmetry, we conclude that there

is always an eigen-energy of 0. Hence there is always an eigen-state at the empty cavity resonance. So if the system is driven resonantly, we should not expect any photon blockade caused only by the anharmonicity of the ladder.

We will now describe the effective model, which is described in the main text only for  $g_a = g_b$  case. To understand the nature of the effect resulting in transmission of sub-Poissonian light, we make the following transformation:

$$\alpha = \frac{g_a a + g_b b}{\sqrt{g_a^2 + g_b^2}} \quad (7)$$

$$\beta = \frac{g_b a - g_a b}{\sqrt{g_a^2 + g_b^2}} \quad (8)$$

Under this transformation, we can rewrite the total Hamiltonian as

$$\mathcal{H} = \mathcal{H}_1 + \mathcal{H}_2 \quad (9)$$

with

$$\mathcal{H}_1 = \Delta(\alpha^\dagger \alpha + \sigma^\dagger \sigma) + \sqrt{g_a^2 + g_b^2}(\alpha \sigma^\dagger + \alpha^\dagger \sigma) + \frac{\mathcal{E}}{\sqrt{1+r^2}}(\alpha + \alpha^\dagger) \quad (10)$$

$$\mathcal{H}_2 = \Delta\beta^\dagger \beta + \frac{r\mathcal{E}}{\sqrt{1+r^2}}(\beta + \beta^\dagger), \quad (11)$$

where  $r = g_b/g_a$ . For  $g_a = g_b$ , we recover the result reported in the main text. When  $r \rightarrow 0$ , there is no light in the uncoupled cavity, and all the light output is from the coupled QD-cavity system. That light is super-Poissonian due to photo-induced tunneling. On the other hand, when  $r \rightarrow \infty$ , the coupled QD-cavity does not get any light. Hence the output light is just in a coherent state, which means its photon statistics will be Poissonian.

### **Light from the undriven cavity mode:**

Here, we briefly discuss the light state from the undriven cavity mode  $b$ . Mode  $b$  is not directly coupled to mode  $a$ , and the only way it can get light is via the QD. Hence the amount of light collected from mode  $b$  is very small, but the light is sub-Poissonian. However, there is no photon blockade present in the mode  $b$ , and the sub-Poissonian character of light in mode  $b$  is similar to the single photons generated by resonant excitation of a QD. Fig. 5 a,b shows the transmitted cavity output and second order auto-correlation  $g^2(0)$  as a function of  $g$  and  $\kappa$ .

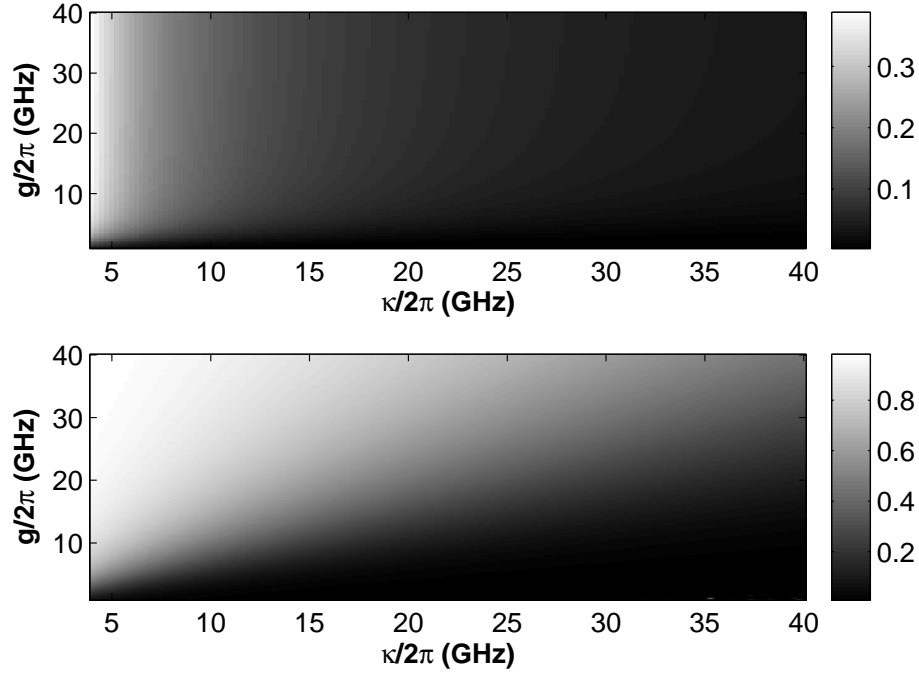


FIG. 5: (a) Transmitted output  $\kappa\langle b^\dagger b \rangle$  from the undriven cavity mode  $b$  as a function of  $g$  and  $\kappa$ . For both the modes same  $g$  and  $\kappa$  are assumed. (b) Second order auto-correlation  $g^2(0)$  for the bimodal cavity as a function of  $g$  and  $\kappa$ . The light is always sub-Poissonian, and results form the resonant QD excitation via mode  $a$ , and collection of the output photons via mode  $b$ . This is similar to a conventional single photon source under resonant excitation of the QD.

### Comparison with the photonic molecule coupled to a quantum dot:

Our method for is somewhat related to the recent proposals of generation of sub-Poissonian light in a photonic molecule [13, 14]. In that approach, one needs two cavities coupled to each other, with one of the cavities containing a weakly coupled QD. The empty cavity is driven, and light is also collected from the empty cavity. Similarly to our bimodal cavity proposal, sub-Poissonian light is obtained when the driving laser is resonant with the system. The Hamiltonian  $\mathcal{H}$  for such a photonic molecule is

$$\mathcal{H} = \Delta(a^\dagger a + \sigma^\dagger \sigma + b^\dagger b) + g(b^\dagger \sigma + b \sigma^\dagger) + J(a^\dagger b + a b^\dagger) + \mathcal{E}(a + a^\dagger) \quad (12)$$

where  $J$  is the cavity-cavity interaction strength. Figure 6 a,b shows the transmitted cavity output and  $g^2(0)$  for two different cases: photonic molecule and the bimodal cavity. We observe that the performance for both the cases are comparable. However, for photonic

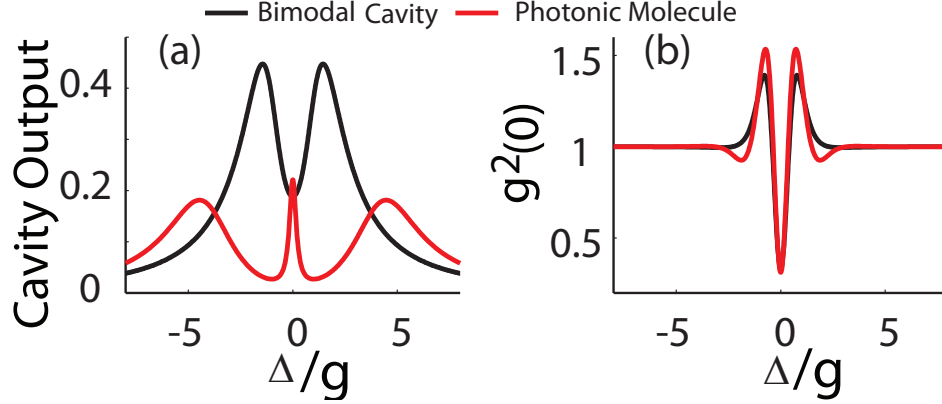


FIG. 6: (color online) (a) Cavity transmitted output for two cases: bimodal cQED and photonic molecule. (b) Second order autocorrelation  $g^2(0)$  for those two cases. Parameters used for the simulations: QD-cavity interaction strengths  $g/2\pi = g_a/2\pi = g_b/2\pi = 10$  GHz; cavity field decay rates  $\kappa_a/2\pi = \kappa/2\pi = 20$  GHz; coupling strength for the Photonic molecule  $J/2\pi = 40$  GHz; dipole decay rate  $\gamma/2\pi = 1$  GHz.

molecule, we need to maintain both individual addressability and high coupling strength between the cavities. In the nano-photonics platform this requirement is challenging, as generally the inter-cavity coupling is achieved by spatial proximity. Although, a wave-guide coupling can be employed to mitigate the problem, that solution brings added complexity of engineering the cavity-to-waveguide coupling. In addition, the cavity output drops if the inter-cavity coupling strength is high, making the photon statistics measurement challenging. On the other hand, our proposal within a bimodal cavity does not require any cavity-cavity coupling. For a degenerate photonic crystal cavity, the two cavity modes are of opposite polarization, and have no coupling. Furthermore, due to orthogonality of their polarizations, each cavity mode can be easily addressed separately as required by the proposal.

### Preliminary experimental result on bimodal photonic crystal cavity:

In this section, we will describe some initial experimental results showing signature of QD-cavity coupling in bimodal cavity, and comment on the feasibility of implementing our theoretical method in this system. Fig. 7 a,b,c show the scanning electron microscope images of three different photonic-crystal cavities designed to support degenerate cavity modes. Fig 7d shows the photoluminescence (PL) spectrum from an  $H1$  (Fig. 7 a) cavity. We have so far

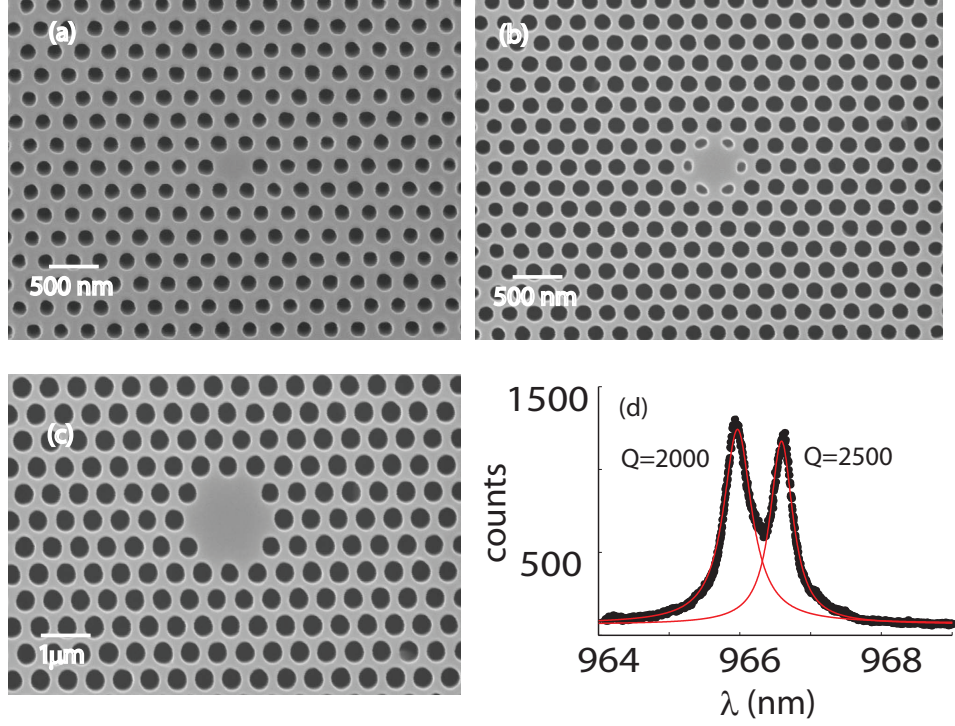


FIG. 7: Scanning electron micrographs of fabricated photonic crystal cavities, that can support degenerate modes: (a)  $H1$  cavity, where the central hole is removed; (b) "calzone" cavity, where the central hole and the half of the next layer of holes are removed; (c)  $H2$  cavity, where the central hole and the first layer of surrounding holes are removed. (d) Photoluminescence spectrum of an  $H1$  cavity showing moderate quality factors and moderate degeneracy of the two modes. Black dots correspond to experimental data points; the red lines are Lorentzian fits.

achieved quality factors of 2000 – 2500 with this cavity design while maintaining significant overlap between the two modes. For this particular system the separation between the two peaks is  $\sim 0.5$  nm.

Lastly, we study the effects of the drive laser polarization to verify that the QD can couple to both cavity modes, and to examine the polarization properties of the two cavity modes. Fig. 8a,b show the PL spectrum of the bimodal cavity system (mode M1 and M2), with a coupled QDs (D1) at two different temperature 20 and 30K. Fig. 8c,d show the polarization dependence of the two modes and the QD. At both temperatures, the cavities are of orthogonal polarizations. However, in Fig. 8c the QD D1, mostly follows the cavity mode M1. With increasing temperature, the QD moves closer to mode M2, and the

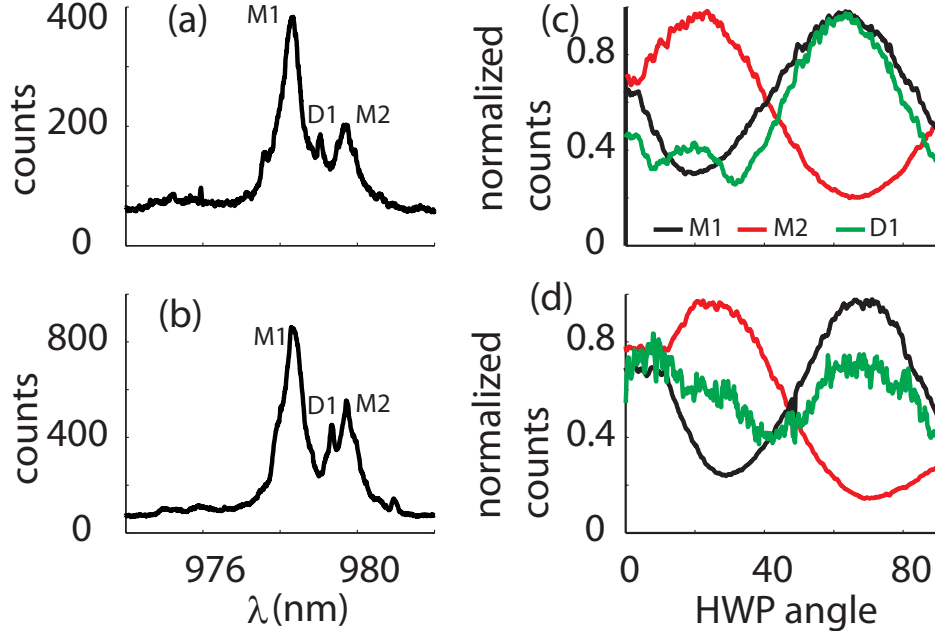


FIG. 8: (color online) (a), (b) PL spectrum of the bimodal cavity (H2 cavity) and a coupled QD at two different temperatures 20K and 30K. The two modes are denoted as M1 and M2 and the QD is denoted as D1. (c),(d) Polarization dependence of the cavity modes (red and black plot) and the QD (green plot) at two different temperatures.

polarization dependence of D1, follows both mode M1 and M2 (Fig. 8d).

Based on these preliminary results, we expect that modest fabrication improvements increasing the frequency overlap of the two modes or or implementation of in-situ frequency tuning of the two modes will allow us to implement the proposed scheme.

---

\* Electronic address: [arkam@stanford.edu](mailto:arkam@stanford.edu)

- [1] A. Majumdar, D. Englund, M. Bajcsy, and J. Vučković, arXiv:1110.4538 (2011).
- [2] D. Englund, A. Majumdar, M. Bajcsy, A. Faraon, P. Petroff, and J. Vučković, arXiv:1107.2956 (2011).
- [3] I. Fushman, D. Englund, A. Faraon, N. Stoltz, P. Petroff, and J. Vuckovic, Science **320** (2008).
- [4] K. M. Birnbaum, A. Boca, R. Miller, A. D. Boozer, T. E. Northup, and H. J. Kimble, Nature **436**, 87 (2005).
- [5] A. Faraon, I. Fushman, D. Englund, N. Stoltz, P. Petroff, and J. Vuckovic, Nature Physics **4**,

- 859 (2008).
- [6] A. Majumdar, M. Bajcsy, and J. Vučković, arXiv:1106.1926 (2011).
  - [7] A. Reinhard, T. Volz, M. Winger, A. Badolato, K. J. Hennessy, E. L. Hu, and A. Imamoglu, arXiv:1108.3053v1 (2011).
  - [8] S. Rosenblum, S. Parkins, and B. Dayan, Phys. Rev. A **84**, 033854 (2011), URL <http://link.aps.org/doi/10.1103/PhysRevA.84.033854>.
  - [9] M. J. Hartmann, F. G. S. L. Brandao, and M. B. Plenio, Nature Physics **2**, 849 (2006).
  - [10] A. D. Greentree, C. Tahan, J. H. Cole, and L. C. L. Hollenberg, Nature Physics **2**, 856 (2006).
  - [11] I. Carusotto, D. Gerace, H. E. Tureci, S. De Liberato, C. Ciuti, and A. Imamoglu, Phys. Rev. Lett. **103**, 033601 (2009), URL <http://link.aps.org/doi/10.1103/PhysRevLett.103.033601>.
  - [12] A. Imamoglu, H. Schmidt, G. Woods, and M. Deutsch, Physical Review Letters **79**, 1467 (1997).
  - [13] T. C. H. Liew and V. Savona, Phys. Rev. Lett. **104**, 183601 (2010), URL <http://link.aps.org/doi/10.1103/PhysRevLett.104.183601>.
  - [14] M. Bamba, A. Imamoglu, I. Carusotto, and C. Ciuti, Phys. Rev. A **83**, 021802 (2011), URL <http://link.aps.org/doi/10.1103/PhysRevA.83.021802>.
  - [15] D. Gerace, H. E. T. A. Imamoglu, V. Giovannetti, and R. Fazio, Nature Physics **281 - 284**, 5 (2009).
  - [16] S. M. Tan, Journal of Optics B: Quantum and Semiclassical Optics **1**, 424 (1999), URL <http://stacks.iop.org/1464-4266/1/i=4/a=312>.
  - [17] G. S. Agarwal and K. Tara, Phys. Rev. A **46**, 485 (1992), URL <http://link.aps.org/doi/10.1103/PhysRevA.46.485>.
  - [18] A. Zavatta, S. Viciani, and M. Bellini, Science **306**, 660 (2004).
  - [19] K. Hennessy, C. Hogerle, E. Hu, A. Badolato, and A. Imamoglu, Appl. Phys. Lett. **89**, 041118 (pages 3) (2006).